Controls on metal leaching from secondary Pb smelter air-pollution-control residues

SUPPORTING INFORMATION

Vojtěch ETTLER[1]*, Ondřej ŠEBEK[2], Tomáš GRYGAR[3],
Mariana KLEMENTOVÁ[3], Petr BEZDIČKA[3]
and Halka SLAVÍKOVÁ[1,4]

1. Institute of Geochemistry, Mineralogy and Mineral Resources, Charles University, Albertov 6, 128 43 Prague 2, Czech Republic (*corresponding author, e-mail: ettler@natur.cuni.cz, tel: +420 221 951 493, fax: +420 221 951 496)
2. Laboratories of Geological Institutes, Charles University, Albertov 6, 128 43, Prague 2, Czech Republic
3. Institute of Inorganic Chemistry, Academy of Science of the Czech Republic, 250 68 Řež, Czech Republic
4. Centre for Waste Management (CWM), T.G. Masaryk Water Research Institute, Podbabská 30, 160 62, Prague 6, Czech Republic

Content: 10 pages, 1 figure, 4 tables

Flue gas cleaning and production of APC residues

Lead (Pb) in the secondary Pb smelter (Kovohutě Příbram, Czech Republic) is obtained by pyrometallurgical processing of Pb scrap, mainly used car batteries. Prior to fusion, the car batteries are crushed and separated from residual sulfuric acid and together with plastic castings, are mixed with coke (reducing agent), recycled silicate slag (source of Si), lime (source of Ca), and iron scrap (source of Fe, flux). A well-balanced mixture of these components forms the charge of the blast furnace (called "water-jacket", Varta technology) and is fused at a temperature of ~ 1350°C to produce molten slag (silicate waste product), matte (sulfide waste product) and metallic Pb through a process called "reducing fusion" (*s1*). The subsequent cleaning of the flue gas (Figure S1) consists of a dust collector, three after-burning chambers (used for elimination of residual organic compounds in the flue gas), three parallel bag-type filters and a chimney.

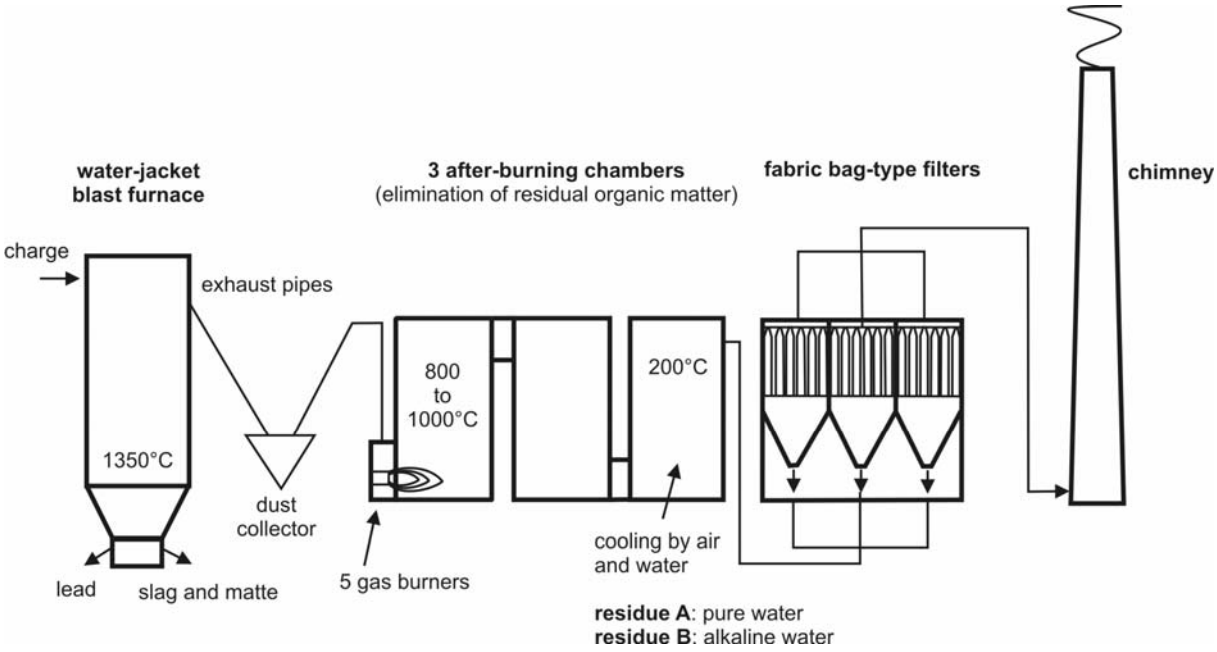

Figure S1. Process scheme of flue gas cleaning in the secondary Pb smelter (modified from (*s1*)).

The flue-gas stream is cooled to 200°C by water sprayed at the level of the third after-burning chamber before entering the bag-house, to prevent destruction of the filters at high temperatures. Through precipitation/condensation processes, the cooling of the flue-gas permitted the formation of fine dust particles, which were subsequently trapped by bag-type filters (called air-pollution-control (APC) residues A and B in this study). Residue A corresponds to a solid trapped by the filters after cooling the flue gas with pure water (Figure S1). In contrast, residue B is a solid trapped by the bag-type filters after cooling the flue gas

with alkaline water (Figure S1). The alkaline water (pH ~ 12) was recycled water originating from the controlled disposal site of alkaline metallurgical slag and is highly enriched in salts (30-40 g Cl L^{-1}, 60-80 g SO_4 L^{-1}, 10 g Na L^{-1}, 10 g CO_3^{2-} L^{-1}) (*s2*).

Although the filtering efficiency is 99.85%, a certain part of the residue can escape from the flue gas cleaning system into the environment and settle *e.g.* in the soil system (*s1*). From a technological point of view, the residue trapped by the bag-type filters is collected and subsequently sintered in a rotary furnace at 300-500°C to reduce the volume and the amount of fine-grained toxic dust in the working area. The obtained residue is subsequently fused with soda (Na_2CO_3) and coke in a rotary furnace to recover more Pb.

Chemical and mineralogical analysis of fresh APC residues

The dissolution/decomposition of APC residues (0.1 g) was performed overnight in closed teflon beakers (Savillex®, Minetonka, USA) in a mixture of 1 ml HNO_3 and 5 ml HF on a hot plate (150°C). The contents of the metallic elements were determined by atomic absorption spectrometry (AAS; Varian SpectrAA 280 FS, Australia) under standard analytical conditions. The NIST 1633b (coal fly ash) and BCR-038 (fly ash from pulverized coal) standard reference materials were used for QC/QA (RSDs for metals < 10 % with respect to certified values). The contents of total inorganic carbon (TIC) and total sulfur (S) in the solid residues were determined by Eltra CS500 and Eltra CS530 C/S analyzers (Germany), respectively. The chloride (Cl) content in the residue digests was determined by inductively coupled plasma optical emission spectroscopy (ICP-OES; Spectro, Spectroflame Modula S, Germany). The dissolution/decomposition procedures and subsequent analyses of metallic elements were performed on 6 replicates (RSD < 7%), while the analyses of TIC and S were performed in triplicate (RSD < 10%).

The mineralogical composition of the APC residues was determined by X-ray diffraction analysis (XRD) using a PANalytical X'Pert Pro diffractometer (conditions: Cu Kα radiation, 40 kV and 30 mA, 2theta range 5-80°, step 0.008, counting time of 350 s using an X'Celerator detector). The qualitative analysis of XRD patterns was performed using the PANalytical X'Pert HighScore software, version 1.0d (PANalytical, the Netherlands) and the ICDD PDF-2 database (*s3*). The quantitative phase composition was calculated by Rietveld analysis using the Diffrac^{plus} Topas software, version 2.1 (Bruker AXS, Germany) and the ICSD database (*s4*). Quantitative estimation of the amorphous components was based on Rietveld analysis of samples spiked with a known amount of standard Si powder (NIST 640c – silicon powder for XRD line position and line profile).

Specifications of speciation-solubility modeling

The PHREEQC-2 speciation-solubility code, version for Windows 2.12.00 (*s5*), was used to determine the metal speciation in extracts and the saturation indices (SI) of possible solubility-controlling phases. All the chemical and physicochemical data (pH, Eh) were entered into the code and the minteq.dat thermodynamic database (derived from MINTEQA2 code; *s6*) was used for all the calculations. The PHREEQC-2 code can be used for ionic strengths up to 0.7 mol L^{-1} (equivalent to sea water) and even higher in Cl-based solutions (*s5*). This was true for the majority of the experimental solutions we obtained. However, very high conductivities were observed for leachates at L/S of 1 L kg^{-1} (both residues) and at L/S of 5 L kg^{-1} (residue B) exceeding 100 mS cm^{-1} (ionic strength > 2 mol L^{-1} as calculated by PHREEQC-2). As the pitzer.dat database suitable for thermodynamic calculations in brines and incorporated into PHREEQC-2 in January 2007 contains no data on Pb and other species, we calculated the entire obtained dataset with minteq.dat, taking into acount that the results of highly concentrated leachates obtained at L/S < 5 L kg^{-1} must be accepted with caution. We tested both databases on calculation of the saturation indices of gypsum ($CaSO_4 \cdot 2H_2O$) according to Hyks et al. (*s6*) for the data points obtained at L/S < 5 L kg^{-1}. The predictions for the degree of gypsum saturation obtained using both databases were very similar (R^2 = 0.91), suggesting that the minteq.dat database can also be used at high ionic strengths.

Metal speciation in leachates

Kinetic leaching test (Table S1). According to our calculations, Pb and Cd were mainly present in the leachates of residue A as chlorocomplexes ($MeCl^+$, $MeCl_2$ and $MeCl_3^-$; up to 85 and 95%, respectively of the total speciation), with minor amounts of free ionic species (up to 27 and 11%, respectively). In contrast, Zn and Cu are mainly present as the free ionic forms (up to 84 and 90% of the total speciation, respectively) with the remainder of the Zn and Cu speciation corresponding to chlorocomplexes. The formation of chlorocomplexes was found to increase the leachability of metals from different contaminated materials (*s8*) and is probably responsible for the high release of Pb and Cd from the studied residues. According to our calculations, , the speciation of Pb and Cd in the leachates of residue B was once again dominated by chlorocomplexes with minor amounts of free ionic forms (up to 15% and 6%, respectively). Sulfate complexes and, in the case of Pb, also carbonate complexes accounted for several % (due to the higher sulfate contents and higher pH and alkalinity of the leachates from residue B). Zinc and Cu were mostly present as the free ionic forms (74 and 88% of the total speciation, respectively), whereas the rest of the speciation corresponded to

chlorocomplexes (up to 39 and 16%, respectively) with minor sulfate and carbonate species (units of %).

Leaching at different L/S ratios (Table S2). For the L/S leaching experiment, the speciation is strictly related to the amount of solubilized salts, with generally higher amounts of Cl complexes at low L/S ratios. The speciation of metals in leachates from residue A is dominated by chloride complexes and free ionic species. This can be summarized as follows (% of chlorocomplexes at L/S of 1000 to L/S of 1): Pb (12-98%), Cu (1-19%), Cd (25-100%) and Zn (1-67% of the total speciation). A very similar contribution of the chlorocomplexes was also observed for the leachates from residue B. However, the speciation at higher L/S ratios was not dominated by free ionic complexes alone, but was also attributed to sulfate complexes (L/S = 1000): Pb (21%), Cu (9%), Cd (11%) and Zn (12% of total speciation).

Possible solubility-controlling phases

Kinetic leaching test (Table S3). Leachates of residue A are oversaturated or close to saturation with respect to anglesite, cotunnite and laurionite. The PHREEQC-2 calculation did not reveal any specific solubility-controlling phases for Zn, Cd and Cu that would be susceptible to precipitation from solution. The leachates of residue B are oversaturated or saturated with respect to phosgenite, laurionite and anglesite and, at the beginning of the experiment, also with respect to cerussite and hydrocerussite. Due to the lack of thermodynamic data for caracolite and $KCl{\cdot}2PbCl_2$, it was not possible to calculate the saturation indices of these phases. In contrast to residue A, additional solubility-controlling phases were suggested by the PHREEQC-2 calculation for other released metals. The B leachates were oversaturated with respect to otavite ($CdCO_3$) and close to saturation with respect to smithsonite ($ZnCO_3$) and $ZnCO_3{\cdot}H_2O$. No Cu-solubility controlling phase was proposed by PHREEQC-2. It is, however, important to recall that no such phase was confirmed in the leached residues by mineralogical methods.

Leaching at different L/S ratios (Table S4). Over the whole range of L/S, the leachates were saturated with respect to anglesite, whereas other Pb-bearing phases were generally saturated at lower L/S ratios. The principal solubility-controlling phases for Cd and Zn could be otavite ($CdCO_3$) and smithsonite ($ZnCO_3$), respectively, in the leachates from residue B (due to the higher pH of the solutions). However, these phases were not confirmed by the mineralogical study and, if present in the leached residues, they are assumed to be present only in trace amounts (below the detection limit of XRD, about 1%).

Table S1. Speciation of metallic contaminants in leachates as calculated by PHREEQC-2 (kinetic leaching test at L/S = 10).

Residue A	Time of leaching (hours)								
	0.5	1	2	12	24	48	168	360	720
Zinc									
Chlorocomplexes*	17.6	19.0	20.9	22.0	23.2	23.6	24.4	18.3	15.2
Zn^{2+}	81.4	79.7	77.6	76.3	74.7	74.1	73.1	80.7	84.1
$ZnSO_4$	0.4	0.4	0.3	0.3	0.3	0.3	0.3	0.3	0.3
$Zn(SO_4)_2^{2-}$	0.0	0.0	0.0	0.0	0.0	0.0	0.0	0.0	0.0
Cadmium									
Chlorocomplexes*	90.7	91.8	93.0	93.6	94.2	94.4	94.8	91.3	88.6
Cd^{2+}	9.3	8.2	7.0	6.4	5.8	5.6	5.2	8.7	11.3
$CdSO_4$	0.1	0.0	0.0	0.0	0.0	0.0	0.0	0.0	0.1
Copper									
Chlorocomplexes*	11.3	12.0	13.0	13.5	14.2	14.5	15.0	11.4	9.7
Cu^{2+}	88.4	87.7	86.8	86.3	85.6	85.4	84.8	88.4	90.1
$CuSO_4$	0.3	0.2	0.2	0.2	0.2	0.2	0.2	0.2	0.2
Lead									
Chlorocomplexes*	76.0	78.2	80.7	81.9	83.3	83.8	84.5	77.3	72.4
Pb^{2+}	23.7	21.5	19.1	17.9	16.5	16.1	15.3	22.5	27.4
$PbSO_4$	0.3	0.3	0.2	0.2	0.1	0.2	0.1	0.2	0.3
Residue B	Time of leaching (hours)								
	0.5	1	2	12	24	48	168	360	720
Zinc									
Chlorocomplexes*	29.0	31.1	33.0	31.9	37.3	37.7	39.3	30.7	21.6
Zn^{2+}	63.4	63.3	62.3	63.9	58.7	58.3	56.8	65.1	73.5
$ZnSO_4$	5.6	4.0	4.0	3.8	3.6	3.6	3.6	3.8	4.4
$Zn(SO_4)_2^{2-}$	0.3	0.2	0.2	0.2	0.1	0.1	0.2	0.2	0.2
$ZnHCO_3^+$	1.7	1.5	0.5	0.3	0.2	0.2	0.2	0.3	0.3
Cadmium									
Chlorocomplexes*	96.2	96.6	97.0	96.8	97.6	97.6	97.8	96.7	94.0
Cd^{2+}	3.2	3.0	2.7	2.9	2.2	2.1	1.9	3.0	5.5
$CdSO_4$	0.5	0.3	0.3	0.3	0.2	0.2	0.2	0.3	0.5
$CdHCO_3^+$	0.1	0.1	0.0	0.0	0.0	0.0	0.0	0.0	0.0
Copper									
Chlorocomplexes*	11.4	13.1	13.7	13.4	15.3	15.3	15.7	12.7	9.8
Cu^{2+}	74.6	81.4	82.6	83.9	82.4	82.3	82.0	84.8	87.6
$CuSO_4$	2.4	1.9	1.9	1.8	1.8	1.8	1.8	1.8	2.0
$CuCO_3$	7.2	2.7	1.0	0.4	0.3	0.3	0.3	0.3	0.3
$Cu(OH)_2$	4.4	0.8	0.8	0.5	0.2	0.3	0.3	0.4	0.3
Lead									
Chlorocomplexes*	77.2	84.2	87.8	88.1	90.7	90.9	91.5	88.0	80.9
Pb^{2+}	8.8	8.9	8.5	9.1	7.2	7.0	6.5	9.2	15.1
$PbSO_4$	2.6	1.9	1.9	1.9	1.6	1.6	1.5	2.0	2.9
$PbCO_3$	9.2	3.2	1.1	0.5	0.3	0.3	0.3	0.4	0.5
$PbHCO_3^+$	2.2	1.8	0.7	0.4	0.3	0.3	0.3	0.4	0.5

* The chlorocomplexes are $MeCl^+$, $MeCl_2$, $MeCl_3^-$, $MeCl_4^{2-}$ where "Me" indicates metal

Table S2. Speciation of metallic contaminants in leachates as calculated by PHREEQC-2 (leaching test at different L/S, time 48 hours).

Residue A	L/S ratio						
	1	5	10	50	100	500	1000
Zinc							
Chlorocomplexes*	65.9	33.7	25.6	8.4	6.1	1.7	1.0
Zn^{2+}	33.2	65.2	74.1	91.5	93.8	98.0	98.6
$ZnSO_4$	0.8	0.8	0.3	0.1	0.1	0.2	0.3
$Zn(SO_4)_2^{2-}$	0.0	0.0	0.0	0.0	0.0	0.0	0.0
$ZnHCO_3^+$	0.1	0.2	0.0	0.0	0.0	0.0	0.1
Cadmium							
Chlorocomplexes*	99.5	96.8	94.4	77.4	70.1	37.8	25.2
Cd^{2+}	0.4	3.1	5.6	22.6	29.9	62.0	74.4
$CdSO_4$	0.4	0.1	0.0	0.0	0.0	0.0	0.0
$CdHCO_3$	0.0	0.0	0.0	0.0	0.0	0.0	0.1
Copper							
Chlorocomplexes*	18.9	15.2	14.5	6.2	4.9	1.5	0.9
Cu^{2+}	80.6	84.3	85.4	93.7	95.1	98.3	98.8
$CuSO_4$	0.5	0.4	0.2	0.0	0.1	0.2	0.2
$CuCO_3$	0.0	0.0	0.0	0.0	0.0	0.0	0.0
$Cu(OH)_2$	0.0	0.0	0.0	0.0	0.0	0.0	0.0
Lead							
Chlorocomplexes*	98.0	89.5	83.8	56.0	47.4	19.8	12.1
Pb^{2+}	1.6	9.8	16.1	43.9	52.5	79.6	86.7
$PbSO_4$	0.3	0.4	0.2	0.1	0.1	0.4	0.6
$PbCO_3$	0.0	0.0	0.0	0.0	0.0	0.0	0.1
$PbHCO_3^+$	0.1	0.3	0.0	0.0	0.0	0.1	0.5
Residue B	L/S ratio						
	1	5	10	50	100	500	1000
Zinc							
Chlorocomplexes*	99.7	47.3	37.7	2.6	3.3	1.4	0.9
Zn^{2+}	0.3	33.0	58.3	77.6	57.3	78.6	87.0
$ZnSO_4$	0.0	15.7	3.6	15.9	33.6	19.1	11.7
$Zn(SO_4)_2^{2-}$	0.0	3.3	0.1	3.5	5.6	0.7	0.2
$ZnHCO_3^+$	0.0	0.7	0.2	0.4	0.2	0.2	0.2
Cadmium							
Chlorocomplexes*	100.0	98.1	97.6	34.1	55.0	32.9	22.6
Cd^{2+}	0.0	0.3	2.1	59.2	26.8	52.2	66.7
$CdSO_4$	0.0	1.6	0.2	6.4	18.1	14.8	10.6
$CdHCO_3^+$	0.0	0.1	0.0	0.3	0.1	0.1	0.1
Copper							
Chlorocomplexes*	25.7	11.8	15.3	2.1	2.9	1.3	0.8
Cu^{2+}	61.2	78.2	82.3	83.7	69.8	81.5	88.1
$CuSO_4$	0.5	7.9	1.8	11.5	26.1	15.0	9.3
$CuCO_3$	12.1	1.7	0.3	0.9	0.4	0.4	0.4
$Cu(OH)_2$	0.5	0.3	0.3	1.8	0.8	1.8	1.4
Lead							
Chlorocomplexes*	93.5	84.8	90.9	18.0	25.2	13.9	9.4
Pb^{2+}	0.0	1.0	7.0	59.7	31.7	54.3	67.7
$PbSO_4$	0.2	10.5	1.6	17.9	41.6	30.0	20.9
$PbCO_3$	6.0	2.5	0.3	2.6	0.8	1.0	1.1
$PbHCO_3^+$	0.4	1.2	0.3	1.8	0.7	0.7	0.9

* The chlorocomplexes are $MeCl^+$, $MeCl_2$, $MeCl_3^-$, $MeCl_4^{2-}$ where "Me" indicates metal

Table S3. Saturation indices of possible solubility-controlling phases as calculated by PHREEQC-2 (kinetic leaching test at L/S = 10).

Residue A		Time of leaching (hours)								
Phase	Composition	0.5	1	2	12	24	48	168	360	720
Cerussite	$PbCO_3$	nd	nd	nd	nd	nd	nd	nd	nd	nd
Phosgenite	$PbCl_2 \cdot PbCO_3$	nd	nd	nd	nd	nd	nd	nd	nd	nd
Hydrocerussite	$Pb_3(CO_3)_2(OH)_2$	nd	nd	nd	nd	nd	nd	nd	nd	nd
Cotunnite	$PbCl_2$	-0.07	0.00	0.07	0.07	0.10	0.11	0.12	-0.09	-0.11
Anglesite	$PbSO_4$	0.42	0.38	0.27	0.23	0.13	0.18	0.10	0.22	0.40
Laurionite	Pb(OH)Cl	-0.52	-0.31	-0.12	-0.35	-0.42	-0.48	-0.33	-0.33	-0.32
Otavite	$CdCO_3$	nd	nd	nd	nd	nd	nd	nd	nd	nd
Smithsonite	$ZnCO_3$	nd	nd	nd	nd	nd	nd	nd	nd	nd
$ZnCO_3 \cdot H_2O$	$ZnCO_3 \cdot H_2O$	nd	nd	nd	nd	nd	nd	nd	nd	nd
Residue B		Time of leaching (hours)								
Phase	Composition	0.5	1	2	12	24	48	168	360	720
Cerussite	$PbCO_3$	0.74	0.45	0.14	-0.09	-0.35	-0.28	-0.29	-0.15	-0.02
Phosgenite	$PbCl_2 \cdot PbCO_3$	0.75	0.67	0.53	0.42	0.19	0.32	0.34	0.34	0.41
Hydrocerussite	$Pb_3(CO_3)_2(OH)_2$	0.50	-0.67	-1.18	-1.71	-2.63	-2.36	-2.42	-1.92	-1.56
Cotunnite	$PbCl_2$	-1.90	-1.70	-1.52	-1.40	-1.37	-1.31	-1.29	-1.42	-1.48
Anglesite	$PbSO_4$	-0.65	-0.63	-0.48	-0.36	-0.44	-0.39	-0.39	-0.34	-0.12
Laurionite	Pb(OH)Cl	-0.06	-0.24	-0.10	-0.08	-0.25	-0.16	-0.17	-0.13	-0.11
Otavite	$CdCO_3$	2.22	1.78	1.37	1.09	0.82	0.87	0.91	1.16	1.32
Smithsonite	$ZnCO_3$	-0.24	-0.59	-0.96	-1.25	-1.44	-1.38	-1.34	-1.24	-1.28
$ZnCO_3 \cdot H_2O$	$ZnCO_3 \cdot H_2O$	0.01	-0.34	-0.71	-1.00	-1.19	-1.13	-1.09	-0.99	-1.03

nd - not determined/not calculated

Table S4. Saturation indices of possible solubility-controlling phases as calculated by PHREEQC-2 (leaching test at different L/S, time 48 hours).

Residue A		L/S ratio						
Phase	Composition	1	5	10	50	100	500	1000
Cerussite	$PbCO_3$	-0.85	0.17	nd	nd	nd	-0.48	-0.09
Phosgenite	$PbCl_2 \cdot PbCO_3$	1.59	2.30	nd	nd	nd	-0.70	-1.09
Hydrocerussite	$Pb_3(CO_3)_2(OH)_2$	-5.69	-1.96	nd	nd	nd	-2.58	-1.71
Cotunnite	$PbCl_2$	0.53	0.22	0.11	-0.08	-0.52	-2.13	-2.91
Anglesite	$PbSO_4$	0.69	0.55	0.18	0.27	0.24	0.09	0.01
Laurionite	Pb(OH)Cl	-0.34	0.35	-0.48	-0.05	-0.14	-0.48	-0.83
Otavite	$CdCO_3$	0.12	0.64	nd	nd	nd	-1.25	-0.84
Smithsonite	$ZnCO_3$	-2.60	-2.14	nd	nd	nd	-4.98	-4.66
$ZnCO_3 \cdot H_2O$	$ZnCO_3 \cdot H_2O$	0.85	-0.29	1.51	0.92	0.78	-0.71	-1.30
Residue B		L/S ratio						
Phase	Composition	1	5	10	50	100	500	1000
Cerussite	$PbCO_3$	3.24	1.29	-0.28	0.39	-0.03	-0.04	-0.04
Phosgenite	$PbCl_2 \cdot PbCO_3$	6.09	2.58	0.32	-0.15	-0.91	-1.81	-2.24
Hydrocerussite	$Pb_3(CO_3)_2(OH)_2$	6.84	1.62	-2.36	-0.05	-1.33	-1.04	-1.06
Cotunnite	$PbCl_2$	0.94	-0.63	-1.31	-2.17	-2.79	-3.68	-4.11
Anglesite	$PbSO_4$	0.91	1.04	-0.39	1.01	0.83	0.57	0.43
Laurionite	Pb(OH)Cl	2.04	0.59	-0.16	-0.24	-0.63	-0.92	-1.16
Otavite	$CdCO_3$	3.94	2.36	0.87	0.78	0.68	0.19	-0.10
Smithsonite	$ZnCO_3$	-0.07	-0.54	-1.38	-4.11	-2.44	-3.08	-3.44
$ZnCO_3 \cdot H_2O$	$ZnCO_3 \cdot H_2O$	0.56	-0.51	-0.91	-2.11	-2.26	-2.72	-2.55

nd - not determined/not calculated

References

(s1) Ettler, V.; Johan, Z.; Baronnet, A.; Jankovský, F.; Gilles, C.; Mihaljevič, M.; Šebek, O.; Strnad, L.; Bezdička, P. Mineralogy of air-pollution-control residues from a secondary lead smelter: environmental implications. *Environ. Sci. Technol.* **2005**, *39*, 9309-9316.

(s2) Ettler, V.; Mihaljevič, M.; Šebek, O.; Strnad, L. Leaching of APC residues from secondary Pb metallurgy using single extraction tests: the mineralogical and the geochemical approach. *J. Hazard. Mater.* **2005**, *B121*, 149-157.

(s3) ICDD. *PDF-2 Database, Release 2002*; International Centre for Diffraction Data: Newton Square, PA, 2002.

(s4) ICSD. *ICSD Database, Release 2005/1*; FIZ-Fachinformationszentrum: Karlsruhe, Germany, 2005.

(s5) Parkhurst, D.L.; Appelo, C.A.J. *User's Guide to PHREEQC (version 2) – a Computer Program for Speciation, Batch-Reaction, One-Dimensional Transport and Inverse Geochemical Calculations;* U.S. Geological Survey report 99-4259: Denver, CO, 1999.

(s6) Allison, J.D.; Brown, D.S.; Novo-Gradac, K.J. *MINTEQA2/PRODEFA2, A Geochemical Assessment Model for Environmental Systems, Version 3.00 User´s Manual and Version 3.11 databases;* EPA/600/3-91/021, U.S. Environmental Protection Agency: Athens, GA, 1991.

(s7) Hyks, J.; Astrup, T.; Christensen, T.H. Influence of test conditions on solubility controlled leaching predictions from air-pollution-control residues. *Waste Manage. Res.* **2007**, *25*, 457-466.

(s8) van der Sloot, H.A.; Comans, R.N.J.; Hjelmar, O. Similarities in the leaching behaviour of trace contaminants from waste, stabilized waste, construction materials and soils. *Sci. Tot. Environ* **1996**, *178*, 111-126.